Zinc Porphyrins Possessing Three p-Carboxyphenyl Groups: Effect of the Donor Strength of Push-Groups on the Efficiency of Dye Sensitized Solar Cells

Authors:

Ram B. Ambre, Sandeep B. Mane, Chen-Hsiung Hung

Abstract:

Zinc porphyrins decorated with three p-carboxyphenyl anchoring groups and various "push" substituents of varied electron-donating strengths were prepared in good yields by facile and straightforward ways. The effect of electron-donating strength of the donor molecules on the overall power conversion efficiency was evaluated with the help of photophysical, electrochemical, photovoltaic spectroscopy and quantum chemical calculations. It is observed from the photophysical and Infrared (IR) spectroscopic data that multi-anchoring dyes are more stable and bind more strongly to the TiO? surface than their one-anchor counterparts. The properties like a three-step synthesis, high overall yields, possible mass production on a gram-scale and strong binding affinities with TiO? surfaces make them a suitable choice for commercial applications. Zn?NH?A, with electron donating and anti-aggregation characteristics, achieved the highest efficiency of 6.50%.

Record Type: Published Article

Submitted To: LAPSE (Living Archive for Process Systems Engineering)

Article

Zinc Porphyrins Possessing Three *p*-Carboxyphenyl Groups: Effect of the Donor Strength of Push-Groups on the Efficiency of Dye Sensitized Solar Cells

Ram B. Ambre, Sandeep B. Mane and Chen-Hsiung Hung *

Institute of Chemistry, Academia Sinica, Nankang, Taipei 11528, Taiwan; rambambre@yahoo.com (R.B.A.); sandmane@gmail.com (S.B.M.)

* Correspondence: chhung@gate.sinica.edu.tw; Tel.: +886-2-2789-8570

Abstract: Zinc porphyrins decorated with three *p*-carboxyphenyl anchoring groups and various "push" substituents of varied electron-donating strengths were prepared in good yields by facile and straightforward ways. The effect of electron-donating strength of the donor molecules on the overall power conversion efficiency was evaluated with the help of photophysical, electrochemical, photovoltaic spectroscopy and quantum chemical calculations. It is observed from the photophysical and Infrared (IR) spectroscopic data that multi-anchoring dyes are more stable and bind more strongly to the TiO_2 surface than their one-anchor counterparts. The properties like a three-step synthesis, high overall yields, possible mass production on a gram-scale and strong binding affinities with TiO_2 surfaces make them a suitable choice for commercial applications. Zn_1NH_3A, with electron donating and anti-aggregation characteristics, achieved the highest efficiency of 6.50%.

1. Introduction

The constantly growing global energy demand is stimulating scientists to pursue alternative energy supplies. Among all renewable energy technologies, solar photovoltaics are believed to be the most encouraging ones as solar energy is the most abundant, lavish, and promising energy source on Earth. Since first reported in 1991, dye sensitized solar cells (DSSCs) have attracted great attention due to their low cost and environmental friendly properties [1]. Among several crucial components of DSSCs, the dye sensitizing molecule is of key importance [1,2]. In the design of an efficient sensitizer, properties like high efficiency, chemical stability, and simple step-economic syntheses play a very important role. The primary role of porphyrins in photosynthetic systems have inspired researchers worldwide to develop highly efficient chromophores based on the porphyrin backbone [3–7]. Porphyrins have emerged as the leaders among DSSCs molecules, with exceptional overall conversion efficiencies of 12%–13% under a push-pull framework [8–11] in competition with ruthenium dyes (11.4%) [12] and organic sensitizers (14.3%) [13–16]. Though efficient, their disadvantages like multistep syntheses, low overall yields and poor stability may hamper their practical applications. Therefore, the search of an efficient porphyrin sensitizer with step-economic synthesis, better overall yield and greater stability is worth pursuing. In DSSCs an anchoring group is necessary to adsorb the dye on a TiO_2 surface, so as to obtain greater stability and fast electron injection [17]. The mode of attachment of sensitizer to the semiconductor surface affects the efficiency of the electron-transfer at the dye-semiconductor interface [18–21]. Organic and phthalocyanine dyes with two anchoring groups are found to be more efficient and stable compared to their single anchoring group counterparts [22,23]. Porphyrins with different anchoring groups through different

binding modes have been used to study their effect on the photovoltaic performance in DSSCs [24–30]. Following our long-term interest in porphyrin-sensitized solar cells [31–38], we have shown that multi-anchoring porphyrins serve as proficient, stable, and cost-effective sensitizers in DSSCs [39–41]. Three-step syntheses, comparatively high overall yields, scalable production, and strong binding with TiO$_2$ surface using two anchoring groups are some of the key features of these porphyrins. An impressive power conversion efficiency >6% is achieved for the devices assembled with these multi-anchoring porphyrins.

Herein we have prepared a series of 1D-π-3A porphyrin sensitizers substituted with a variety of donor molecules with variable electron-donating strengths, as shown in Scheme 1. The nature and strength of the donor groups have significant effects on their photovoltaic performance. These porphyrins were prepared from commercially available starting compounds in just three steps. The overall reaction yields of these porphyrins are in the range of 2%–6% which are comparatively higher than the reported push-pull porphyrins (<1%) [8].
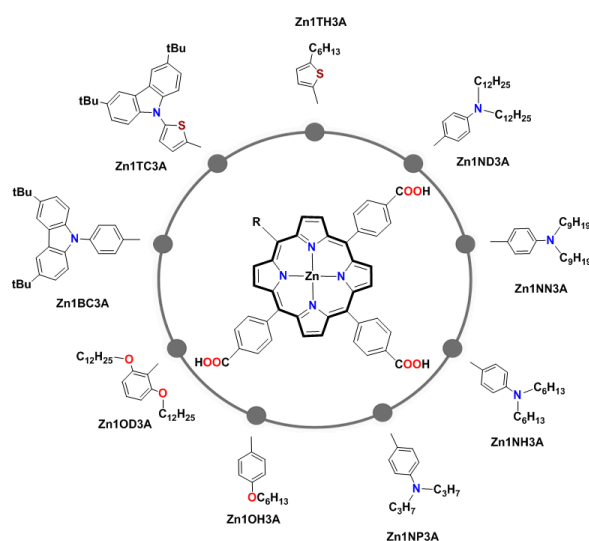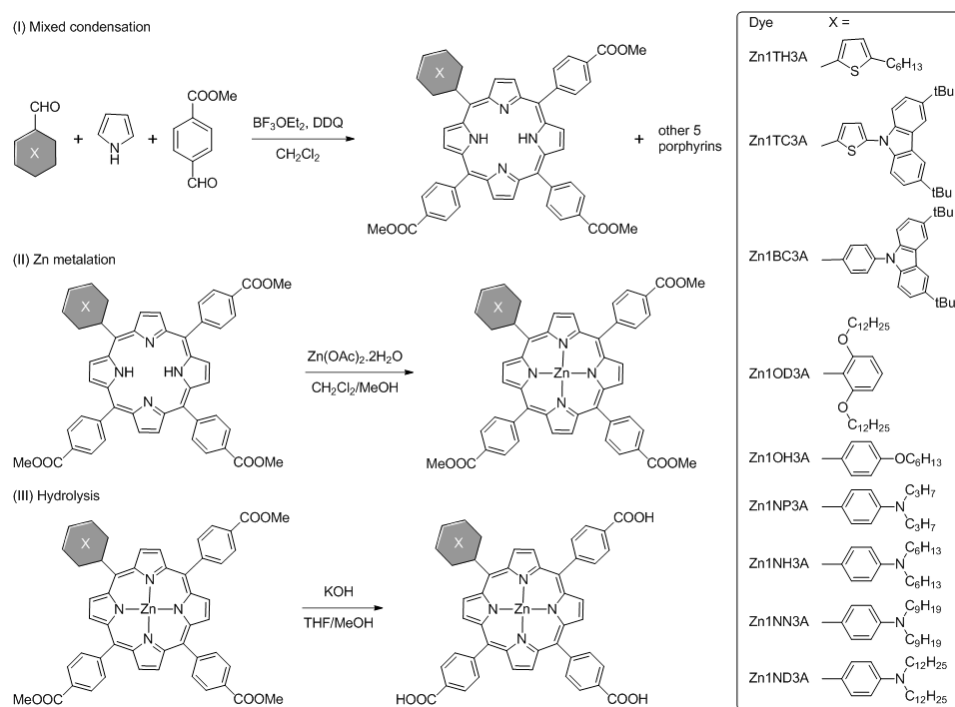

Scheme 1. 1D-π-3A porphyrin sensitizers used in the study.

2. Results and Discussion

2.1. Synthesis

The 1D-π-3A porphyrinic sensitizers were synthesized in three steps, namely mixed condensation, zinc metalation, and base hydrolysis. The detailed synthetic route is presented in Scheme 2. Condensation of pyrrole, methyl-4-formylbenzoate, and the corresponding aldehyde under Lindsey conditions catalysed by boron trifluoride diethyl etherate, followed by subsequent oxidation by 2,3-dichloro-5,6-dicyano-1,4-benzoquinone (DDQ) yielded the triester derivatives in decent yields. In the attenuated total reflectance Fourier transform infrared spectroscopy (ATR-FTIR) spectra all the porphyrins show one stretching frequency at around 1720 cm^{-1} confirming the presence of the ester carbonyl group. In the ultraviolet visible (UV/Vis) spectra the free-base porphyrins show a strong Soret band and four moderate Q bands. The subsequent step of zinc metallation has been readily achieved in high yields by reacting the free-based porphyrin with zinc acetate. The formation of zinc complexes of all the porphyrins was confirmed through the complete disappearance of the nuclear magnetic resonance (NMR) signal of the inner NH protons with slightly upfield shifts for all remaining protons. Hydrolysis of these metal complexes have been achieved straightforwardly by reacting them in a mixture solution of tetrahydrofuran (THF) and methanol with excess aqueous KOH. ATR-FTIR spectra of final acid products show shifting of carbonyl peaks in the range of 1675–1700 cm^{-1} because of intermolecular hydrogen bonding. All of the porphyrins were fully

characterized by optical spectroscopy, ATR-FTIR, nuclear magnetic resonance spectroscopy, and high-resolution mass spectrometry.

Scheme 2. Synthetic route to the studies 1D-π-3A porphyrin sensitizers.

2.2. Photophysical Properties

The UV/Vis absorption spectra of the studied zinc(II) porphyrin dyes, as displayed in Figure 1, shows one strong Soret band and two Q bands.
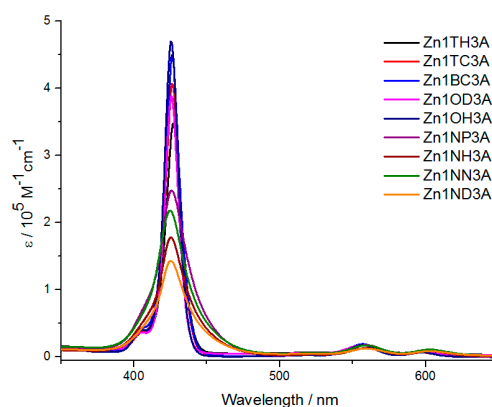
Figure 1. Ultraviolet visible (UV/Vis) spectra of the 1D-π-3A porphyrin sensitizers in tetrahydrofuran.

The peak positions and their molar absorption coefficients (ε) are summarized in Table 1. The shift in absorption bands of porphyrins are substituent-dependent. Porphyrin Zn_1TH_3A has the Soret band absorption at 427 nm while Zn_1TC_3A, Zn_1BC_3A, Zn_1OD_3A, Zn_1OH_3A and Zn_1NP_3A display Soret band absorptions at 426 nm. In the cases of porphyrins Zn_1NH_3A, Zn_1NN_3A, and Zn_1ND_3A, the Soret bands shift to 425 nm. The overall highest molar ε has been observed for Zn_1OH_3A. It is interesting to observe that the porphyrins Zn_1TH_3A, Zn_1TC_3A, Zn_1BC_3A, Zn_1OD_3A, and Zn_1OH_3A have relatively high molar ε than the *N,N′*-alkylaniline-substituted porphyrins.

Table 1. Electrochemical Properties of studied porphyrins.

Dye	λ_{abs} (nm) [1]	λ_{em} (nm) [2]	E_{ox} (V) [3]	E_{0-0} (eV) [4]	E_{ox}* (V) [5]
Zn$_1$TH$_3$A	427 (350)	612	0.93	2.04	−1.11
	558 (18)	656	-	-	-
	600 (9)	-	-	-	-
Zn$_1$TC$_3$A	426 (409)	605	0.94	2.06	−1.12
	558 (17)	654	-	-	-
	599 (6)	-	-	-	-
Zn$_1$BC$_3$A	426 (452)	606	0.91	2.06	−1.15
	557 (19)	658	-	-	-
	598 (7)	-	-	-	-
Zn$_1$OD$_3$A	426 (391)	605	1.06	2.06	−1.00
	557 (18)	657	-	-	-
	597 (7)	-	-	-	-
Zn$_1$OH$_3$A	426 (471)	607	0.97	2.06	−1.09
	557 (18)	656	1.33	-	-
	597 (7)	-	-	-	-
Zn$_1$NP$_3$A	426 (248)	621	0.94	2.03	−1.09
	560 (18)	-	1.06	-	-
	604 (11)	-	-	-	-
Zn$_1$NH$_3$A [6]	425 (178)	622	0.96	2.03	−1.07
	559 (13)	-	1.08	-	-
	603 (8)	-	-	-	-
Zn$_1$NN$_3$A	425 (218)	624	1.01	2.03	−1.02
	559 (17)	-	1.10	-	-
	603 (11)	-	-	-	-
Zn$_1$ND$_3$A [6]	425(143)	624	0.92	2.03	−1.11
	560 (12)	-	1.05	-	-
	603 (8)	-	-	-	-

[1] Absorption maximum ($\varepsilon/10^3$ M$^{-1}\cdot$cm^{-1}) of porphyrin in THF; [2] Emission maximum were measured in THF by exciting at Soret band; [3] First oxidation potentials were determined by cyclic voltammetry in THF; [4] E_{0-0} values were estimated from the intersection of the absorption and emission spectra; [5] E_{ox}* approximated from E_{ox} and E_{0-0}; [6] From reference [40].

Although the molar ε are not high for Zn$_1$NP$_3$A, Zn$_1$NH$_3$A, Zn$_1$NN$_3$A, and Zn$_1$ND$_3$A, the low absorbance might be compensated by the broadened absorption and better electron injection to result in higher overall conversion efficiencies (*vide infra*).To better understand the adsorption behavior of porphyrins on TiO$_2$, the thin film absorption spectra of these porphyrins were studied. The UV/Vis spectra of studied porphyrins on TiO$_2$ displayed in Figure 2 shows slightly red-shifted absorption wavelengths with broadening in shape.
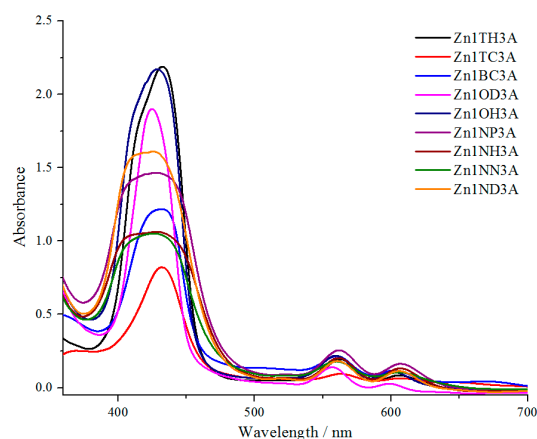
Figure 2. UV/Vis spectra of the 1D-π-3A porphyrin sensitizers adsorbed on TiO$_2$.

The absorption wavelengths of porphyrins Zn_1TH_3A, Zn_1TC_3A and Zn_1BC_3A adsorbed on TiO_2 are red-shifted by 5 nm with slight broadening in shape, forming J-aggregates on TiO_2 by end-to-end stacking, whereas in TiO_2 films absorbing the rest of the porphyrins only peak broadening without any shift in the absorption wavelength was observed. The emission spectra of Zn_1TH_3A, Zn_1TC_3A, Zn_1BC_3A, Zn_1OD_3A, and Zn_1OH_3A show two peaks while the other *N,N'*-alkylaniline substituted porphyrins Zn_1NP_3A, Zn_1NH_3A, Zn_1NN_3A, and Zn_1ND_3A show only one peak with a red-shifted emission.

2.3. Electrochemical Properties

To determine the first oxidation potential (E_{ox}) of porphyrins, cyclic voltammetry measurements of the studied porphyrins were performed in degassed THF solution containing 0.1 M tetrabutylammonium hexafluorophosphate (TBAPF$_6$) as electrolyte. Supplementary Material (Figure S1) shows cyclic voltammograms of the porphyrin sensitizers. All of the porphyrins give well resolved and reversible waves for the first oxidation couple which is stable over multiple scans. The values of oxidation potential as listed in Table 1 indicate that the peripheral substituents on the *meso* positions moderately alter the oxidation potentials. A lowest first oxidation potential of 1.06 V has been observed for Zn_1OD_3A. Porphyrins Zn_1TH_3A, Zn_1TC_3A, Zn_1BC_3A, and Zn_1OD_3A gave one reversible oxidation couple while for the remaining porphyrins two reversible oxidation couples were observed. The oxidation potentials of all studied porphyrins are greater than that of I^-/I_3^- couple assuring the regeneration of oxidized dyes. The excited-state oxidation potentials (E_{ox}^*) are obtained from the equation $E_{ox}^* = E_{ox1} - E_{0-0}$ where E_{ox1} is the first oxidation potential of a porphyrin dye and E_{0-0} is the zero-zero excitation energy obtained from the intersection of the absorption and emission spectra. The calculated E_{ox}^* energy levels of these porphyrins depicted in Table 1 are more negative than the conduction band of TiO_2 (−0.50 V versus NHE), exhibiting the sufficient driving force for electron injection from the excited state of the dye to the conduction band (CB) of TiO_2. The systematic energy level diagrams of studied porphyrins are shown in Figure 3 demonstrating feasibility of dye regeneration with electrolyte and electron injection to conduction band.
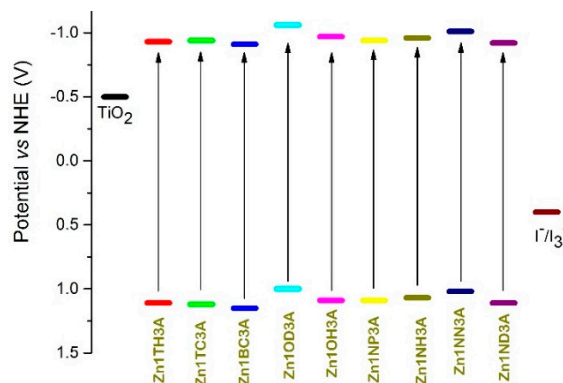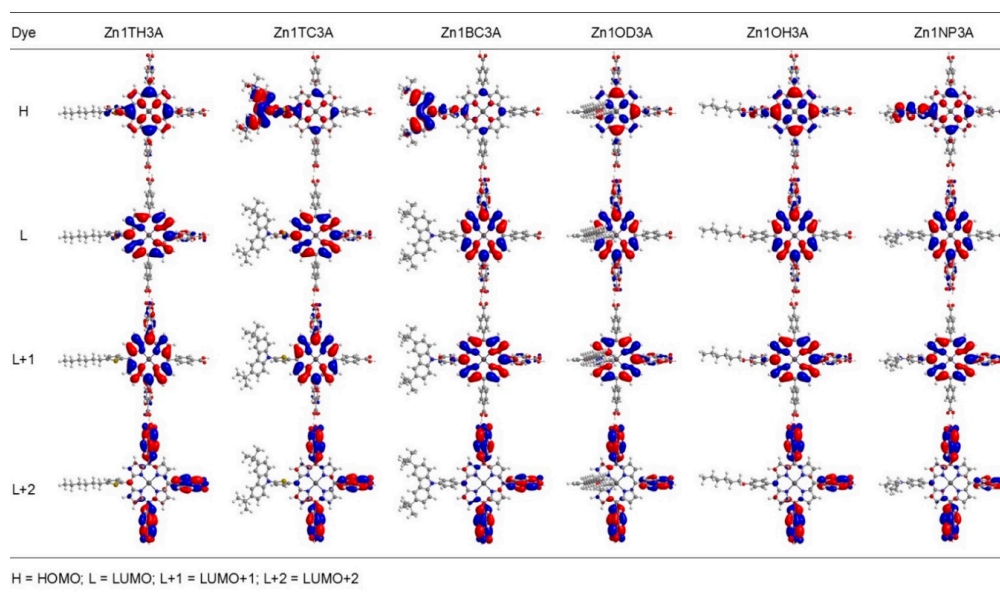

Figure 3. Energy level diagram for 1D-π-3A porphyrin sensitizers.

2.4. Quantum Chemical Results

To gain insights into the electronic structures for the frontier orbitals of the porphyrins, density functional theory calculations were carried out for studied porphyrins at the B3LYP/6-31G(d) level using Gaussian 09 Software [42,43]. Figure 4 illustrates the electron density distributions of studied porphyrins in their respective HOMO, LUMO, LUMO + 1, and LUMO + 2 molecular orbitals.

Analyzing the orbitals in detail, for HOMO orbitals, the electron density distributions for porphyrin dyes varies greatly with the electron-donating tendency of the push group. The electronic cloud density over the HOMO and LUMO estimate the hole and electron carrying ability, respectively [44]. In the studied porphyrins the electron density is mainly localized on the porphyrin core in the HOMO orbitals for Zn_1TH_3A, Zn_1OD_3A, and Zn_1OH_3A, with a small part of it extended

over the weak electron-donating substituent, while the majority of the electron density is localized on the strong electron donating groups has seen for Zn_1TC_1A, Zn_1BC_3A, Zn_1NP_3A, Zn_1NH_3A, Zn_1NN_3A and Zn_1ND_3A. Although the porphyrin core is still the main electron population site, in both LUMO and LUMO+1 orbitals, a significant amount of electron density is distributed over the *meso* carboxyphenyl anchoring group. Interestingly, Zn_1TH_3A, and Zn_1TC_3A have electron density localized at the carboxylphenyl group opposite to the electron donating substituent for LUMO orbitals and at the 5- and 15-carboxyphenyl, the *meso* substituents neighboring the donating group, for LUMO+1 orbitals but a reverse distribution pattern is observed for the rest of the zinc porphyrin dyes. Given that our ATR-IR analyses demonstrate a *cis* two arm anchoring with one dangling carboxyphenyl group for these tricarboxyphenyl-containing porphyrin dyes [39,40], it is likely that the LUMO and LUMO + 1 synchronize to pump electron density into the conduction band of TiO_2.

| Dye | Zn1TH3A | Zn1TC3A | Zn1BC3A | Zn1OD3A | Zn1OH3A | Zn1NP3A |

H = HOMO; L = LUMO; L+1 = LUMO+1; L+2 = LUMO+2

Figure 4. Molecular orbital diagrams of 1D-π-3A porphyrins obtained from density functional theory (DFT) calculations.

Also for the LUMO + 2 orbital all the electron density is exclusively localized on the carboxyphenyl anchoring group, indicating that the electron injection from higher excited states involving the LUMO + 2 orbital is also possible. Nevertheless, it is clearly evident from the electron density distribution that the porphyrin dyes containing a strong electron-donating *meso* substituent provides better charge separation which slows down the charge recombination and results in a more efficient electron injection.

2.5. Photovoltaic Properties

The 1D–π–3A porphyrins were fabricated into solar cell devices in the presence of chenodeoxycholic acid (CDCA) as a co-adsorbent according to the procedures detailed in the Experimental Section and evaluated for the photovoltaic performance under standard AM 1.5 G simulated solar conditions. The best photovoltaic performance for each porphyrin is summarized in Table 2. The optimized *I-V* curves of all the studied three *p*-carboxyphenyl substituted porphyrins are shown in Figure 5. As observed from the photovoltaic data and *I-V* curves, the strong electron-donating *N,N′*-alkylaniline- substituted porphyrins outperform the devices using the rest of the porphyrins as the sensitizer. The Zn1TH3A porphyrin having a hexylthiophene group as electron donor at the *meso*-position exhibits an efficiency of 5.36% based on a short-circuit current density (J_{sc}) of 12.41 mA cm^{-2}, an open-circuit voltage (V_{oc}) of 0.65 V and a fill factor (*FF*) of 67%, whereas the porphyrin dyes Zn1TC3A and Zn1BC3A with carbazole donor groups obtained overall

power conversion efficiencies of 4.49% and 4.40%, respectively. The Zn_1OD_3A porphyrin with an *ortho*-didodecylphenyl substituent on the meso position achieved a conversion efficiency of 4.78%, while the hexyloxyphenyl-substituted porphyrin Zn_1OH_3A attained an overall performance of 4.81%.
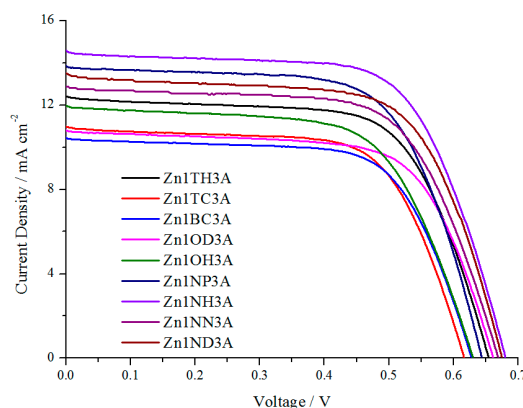

Figure 5. *I-V* curves for 1D-π-3A porphyrin sensitizers.

Table 2. Photovoltaic characteristics of dye sensitized solar cells (DSSCs) incorporating the 1D-π-3A porphyrin dyes. *FF*: fill factor.

| Dye	J_{sc} (mA·cm^{-2})	V_{oc} (V)	*FF* (%)	η (%)	Γ (nmol·cm^{-2})
Zn_1TH_3A	12.41	0.65	67	5.36	102
Zn_1TC_3A	9.95	0.62	67	4.49	135
Zn_1BC_3A	10.45	0.62	68	4.40	132
Zn_1OD_3A	10.80	0.66	66	4.78	90
Zn_1OH_3A	11.98	0.63	64	4.81	125
Zn_1NP_3A	13.86	0.64	66	5.86	140
Zn_1NH_3A	14.55	0.68	65	6.50	138
Zn_1NN_3A	12.87	0.67	65	5.65	126
Zn_1ND_3A	13.50	0.67	66	6.00	137

It is noteworthy that the dye loading for the porphyrin Zn_1OD_3A is 90 nmol·cm^{-2} which is the least among the studied porphyrin dyes due to the presence of two *ortho*-dodecyl side chains, which might hinder close packing of the molecules in TiO$_2$ surface.

The higher efficiency of the Zn_1TH_3A porphyrin than Zn_1TC_3A, Zn_1BC_3A, Zn_1OD_3A and Zn_1OH_3A is most likely because of its stronger electron-donating character, inhibition of charge recombination, and effective charge separation. The *N,N'*-alkylaniline-substituted porphyrin sensitizers Zn_1NP_3A, Zn_1NH_3A, Zn_1NN_3A and Zn_1ND_3A gave efficiencies higher than 5.6%. The intrinsic anti-aggregation properties resulting from the presence of long alkyl chains and electron-donating character have both been instrumental in their superior performance. For comparison we varied the alkyl chain length from propyl, hexyl, nonyl, to dodecyl. The propyl-substituted porphyrin Zn_1NP_3A gave a J_{sc} of 13.86 mA·cm^{-2}, V_{oc} of 0.64 V and *FF* of 66% corresponding to an overall performance of 5.86%. The porphyrin Zn_1NH_3A with hexyl substituent achieved a power conversion efficiency of 6.5%. The nonyl derivative Zn_1NN_3A obtained a power conversion efficiency of 5.65%, while the *N*-dodecyl-decorated porphyrin Zn_1ND_3A gives a J_{sc} of 13.61 mA·cm^{-2} and a moderate V_{oc} of 0.65 V contributed to its efficiency of 6%.

The incident photon-to-current efficiency (IPCE) characteristics of studied porphyrins show similar trends with the observed J_{sc} and are shown in Figure 6. The IPCE values demonstrated at the Soret band region are consistent with the performance of the porphyrin dyes. The highest IPCE value of 81% is observed for Zn_1NH_3A having the highest efficiency of 6.50%, whereas the IPCE value of 40% is observed for Zn_1BC_3A having an efficiency of 4.40%. It is also evident from the IPCE spectra that the *N,N'*-alkylaniline-substituted porphyrins show intense, broad, and red-shifted IPCE absorption

features compared to other porphyrins. The dip around 500–550 nm is also slightly higher for them than the latter. The dye loading of the porphyrins on TiO$_2$ films was examined and summarized in Table 2. The dye densities and efficiencies of porphyrins are roughly consistent; Zn$_1$NH$_3$A has the highest dye loading density giving the highest efficiency whereas, despite a low dye density, Zn$_1$OD$_3$A is able to give good performance (η = 4.78%). It is worth mentioning that a regular desorption solvent, 0.1 M aqueous KOH in THF (2:8, v/v), failed to completely desorb these three *p*-carboxyphenyl substituted sensitizing dyes, even after exposure for 24 h. It requires a solution of 0.2 M KOH(aq) in THF (1:1, v/v) to completely desorb the dye attached onto the TiO$_2$ surface. The use of a high concentration of base to desorb the dye is an additional support to prove the higher stabilities of three *meso p*-carboxyphenyl groups-possessing porphyrins.
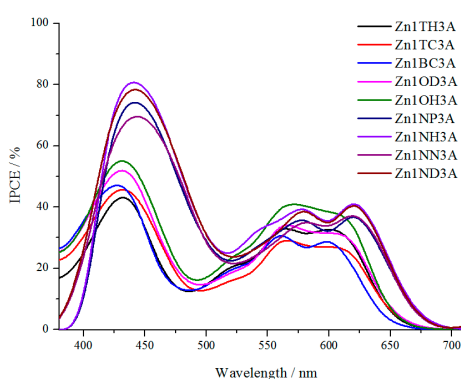
Figure 6. The incident photon-to-current efficiency spectra for 1D-π-3A porphyrin sensitizers.

2.6. Stability Test of Porphyrin Sensitizers

For the commercialization of DSSCs, along with a high efficiency, the long term stability is an important issue to be considered. We have used a simple method to examine the stability of the studied dyes. To obtain the stability information, the absorption spectra of three *p*-carboxyphenyl group-possessing porphyrins Zn$_1$ND$_3$A were compared with that of a single anchoring group possessing porphyrin Zn$_3$TPA$_1$A (Zn$_3$TPA$_1$A possesses three triphenyl amine and one *p*-carboxy-phenyl group on its *meso* positions) upon irradiation. The TiO$_2$ film adsorbed with Zn$_1$ND$_3$A, and Zn$_3$TPA$_1$A were irradiated under standard one-sun illumination and the absorption spectra were monitored after irradiation for 0, 5, and 30 min. The observed results depicted in Figure 7 suggest that the absorbance of dyes decreases at various rates without any shifting of the wavelength of maximum absorbance. The decrease in the absorbance is significantly larger for Zn$_3$TPA$_1$A in comparison with Zn$_1$ND$_3$A which suggests that the porphyrins possessing three *p*-carboxyphenyl groups are more stable compared to porphyrins possessing a single anchoring group.
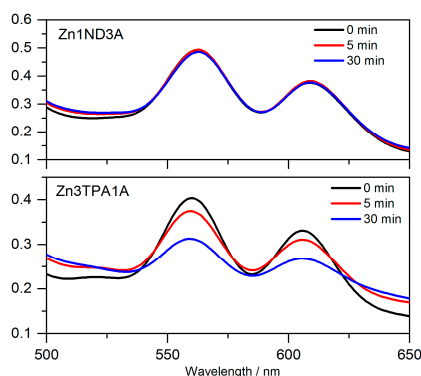
Figure 7. Stability study of Zn$_1$ND$_3$A and Zn$_3$TPA$_1$A.

3. Materials and Methods

3.1. Synthesis

All of the porphyrins were characterized by optical spectroscopy, ATR-FTIR, NMR spectroscopy, and high resolution mass spectrometer (HRMS). All of the chemicals were purchased from Acros Organics (Geel, Belgium) or Sigma Aldrich (St. Louis, MO, USA) and used without further purification. ^{1}H-NMR spectra were recorded on a Bruker 400 MHz spectrometer (Rheinstetten, Germany) in CDCl$_3$ (δ = 7.26 ppm), or DMSO-d$_6$ (δ = 2.50 ppm). Chemical shifts are reported in ppm. coupling constants (*J*) are reported in Hz. The signals are described as s = singlet, d = doublet, t = triplet, or p = pentet. HRMS (fast atom bombardment or electrospray ionization) was performed on a JMS-700 double-focusing mass spectrometer (JEOL, Tokyo, Japan). Flash chromatography was performed on silica gel (40–63 μm, Merck, Darmstadt, Germany). Analytical thin-layer chromatography (TLC) was performed on silica-gel plates (Merck). Melting points were recorded on a capillary melting-point apparatus (Electrothermal, Staffordshire, UK).

3.2. Optical Spectroscopy

UV/Vis absorption spectra of the porphyrins in THF and adsorbed onto TiO$_2$ electrodes were recorded on a V-670 UV/Vis/NIR spectrophotometer (JASCO, Easton, MD, USA). For the absorption spectra of the thin films on TiO$_2$, TiO$_2$ films (area: 1×1 cm^2) were prepared with thicknesses of about 1 μm to obtain comparable shapes and peak positions. The films were immersed in 2×10^{-4} M solutions of the porphyrins in THF for 12 h and the films were rinsed with THF, dried, and the absorbance was measured. Steady-state fluorescence spectra were acquired on a Cary Eclipse fluorescence spectrophotometer (Varian, Palo Alto, CA, USA).

3.3. Cyclic Voltammetry

The cyclic voltammetry (CV) measurements of all of the porphyrins were performed on a CHI 600D electrochemical analyzer (CH Instruments, Austin, TX, USA) in degassed THF with 0.1 M TBAPF$_6$ as a supporting electrolyte. The cell assembly consisted of a glassy carbon working electrode, Ag wire as a reference electrode, and platinum wire as the auxiliary electrode. A ferrocene/ferrocenium redox couple was used as an internal reference.

3.4. Density Functional Theory Calculations

Geometry optimizations and the electronic structures of the porphyrins were performed by using DFT at the B3LYP level of theory with the 6-31G(d) basis set in the Gaussian09 Program Package (Gaussian Inc., Wallingford, CT, USA).

3.5. Photovoltaic Measurements

TiO$_2$ photoanode films were purchased from Yingkou Opvtech New Energy Co., Ltd. (Yingkou Liaoning, China). The films, which were prepared using the screen-printing method, were composed of a transparent layer (thickness $\approx$ 12 μm), a scattering layer (thickness $\approx$ 4 μm), and a working area of 0.4×0.4 cm^2. The films were pretreated according to the following activation procedures before use: heating at 100 °C for 22 min, at 110 °C for 60 min, at 450 °C for 68 min, at 500 °C for 60 min, at 250 °C for 60 min, cooling at 80 °C and keeping at 80 °C before immersion. The TiO$_2$ films were immersed in a 2×10^{-4} M solution of the porphyrin and a 6×10^{-4} M solution of CDCA in THF at 50 °C. The dye-sensitized TiO$_2$ films were washed with THF, dried in hot air, and used as the working electrode. The counter electrode was prepared on an indium-doped tin-oxide glass substrate (typical size: 1.0×1.5 cm^2) by spin-coating a H$_2$PtCl$_6$/isopropanol solution through thermal decomposition at 380 °C for 0.5 h. To fabricate the DSSC device, the two electrodes were tightly clipped together into a sandwich-type cell that was spaced by a 40 μm film spacer. A thin layer of electrolyte, which contained 0.05 M I$_2$, 0.1 M lithium iodide (LiI), 0.6 M dimethyl-propyl-benzimidiazole iodide (DMPII),

and 0.6 M 4-*tert*-butylpyridine (TBP) in dry CH_3CN, was introduced into the space between the two electrodes. The photo-electrochemical characterizations on the solar cells were performed on an Oriel Class A solar simulator (Oriel 91195A, Newport Corp., Andover, MA, USA). Photocurrent-voltage characteristics of the DSSCs were recorded on a potentiostat/galvanostat (CHI650B, CH Instruments, Inc.) at a light intensity of 100 mW·cm^{-2} and calibrated to an Oriel reference solar cell (Oriel 91150). The monochromatic quantum efficiency was recorded on a monochromator (Oriel 74100) under short-circuit conditions. The intensity of each wavelength was within the range 1–3 mW·cm^{-2}.

3.6. Stability Test of Porphyrin Sensitizers

For the stability study, TiO_2 thin films with areas of 1×1 cm^2 and thicknesses of 3–4 μm were used. The films were immersed in a 2×10^{-4} M solution of the porphyrin in THF for 0.5 h, dried, and the absorbance was measured. Then, the same films were irradiated under standard one sun illumination for 5 min and 30 min and the absorbance was measured again.

4. Conclusions

Porphyrins Zn_1TH_3A, Zn_1TC_3A, Zn_1BC_3A, Zn_1OD_3A, Zn_1OH_3A, Zn_1NP_3A, Zn_1NHA, Zn_1NN_3A, and Zn_1ND_3A with *meso*-substituted electron-donating substitutions and three carboxyphenyl groups have been synthesized from readily available starting materials in high yields. The syntheses of the studied sensitizers are facile, straightforward, and scalable. The redox potentials of the studied porphyrins have a significant effect on the photovoltaic properties. ATR-FTIR spectra of the studied three-carboxyphenyl-group-possessing porphyrins on TiO_2 reveal that two *p*-carboxy-phenyls are attached on TiO_2 with a double arm binding mode. Higher than 4% efficiency has been achieved by all of the studied porphyrins. Zn_1NH_3A gives best performance owing to its electron donating and anti-aggregation characteristics. The stability study performed demonstrates the studied multi-anchored porphyrins are more stable compared to its mono-anchored analogs.

Author Contributions: Chen-Hsiung Hung conceived and designed the experiments; Ram B. Ambre and Sandeep M. Mane performed the experiments.

Conflicts of Interest: The authors declare no conflict of interest. The founding sponsors had no role in the design of the study; in the collection, analyses, or interpretation of data; in the writing of the manuscript, and in the decision to publish the results.

References

1.　Hagfeldt, A.; Boschloo, G.; Sun, L.; Kloo, L.; Pettersson, H. Dye-sensitized solar cells. *Chem. Rev.* **2010**, *110*, 6595–6663. [CrossRef] [PubMed]

2.　Gratzel, M. Photoelectrochemical cells. *Nature* **2001**, *414*, 338–344. [CrossRef] [PubMed]

3.　Campbell, W.M.; Burrell, A.K.; Officer, D.L.; Jolley, K.W. Porphyrins as light harvesters in the dye-sensitised TiO_2 solar cell. *Coord. Chem. Rev.* **2004**, *248*, 1363–1379. [CrossRef]

4.　Imahori, H.; Umeyama, T.; Ito, S. Large π-aromatic molecules as potential sensitizers for highly efficient dye-sensitized solar cells. *Acc. Chem. Res.* **2009**, *42*, 1809–1818. [CrossRef] [PubMed]

5.　Martinez-Diaz, M.V.; de la Torre, G.; Torres, T. Lighting porphyrins and phthalocyanines for molecular photovoltaics. *Chem. Commun.* **2010**, *46*, 7090–7108. [CrossRef] [PubMed]

6.　Walter, M.G.; Rudine, A.B.; Wamser, C.C. Porphyrins and phthalocyanines in solar photovoltaic cells. *J. Porphyr. Phthalocyanines* **2010**, *14*, 759–792. [CrossRef]

7.　Li, L.L.; Diau, E.W.G. Porphyrin-sensitized solar cells. *Chem. Soc. Rev.* **2013**, *42*, 291–304. [CrossRef] [PubMed]

8. Bessho, T.; Zakeeruddin, S.M.; Yeh, C.Y.; Diau, E.W.G.; Grätzel, M. Highly efficient mesoscopic dye-sensitized solar cells based on donor–acceptor-substituted porphyrins. *Angew. Chem. Int. Ed.* **2010**, *49*, 6646–6649. [CrossRef] [PubMed]

9. Mathew, S.; Yella, A.; Gao, P.; Humphry-Baker, R.; CurchodBasile, F.E.; Ashari-Astani, N.; Tavernelli, I.; Rothlisberger, U.; Nazeeruddin, K.; Grätzel, M. Dye-sensitized solar cells with 13% efficiency achieved through the molecular engineering of porphyrin sensitizers. *Nat. Chem.* **2014**, *6*, 242–247. [CrossRef] [PubMed]

10. Yella, A.; Lee, H.W.; Tsao, H.N.; Yi, C.; Chandiran, A.K.; Nazeeruddin, M.K.; Diau, E.W.G.; Yeh, C.Y.; Zakeeruddin, S.M.; Grätzel, M. Porphyrin-sensitized solar cells with cobalt (II/III)-based redox electrolyte exceed 12 percent efficiency. *Science* **2011**, *334*, 629–634. [CrossRef] [PubMed]

11. Yella, A.; Mai, C.L.; Zakeeruddin, S.M.; Chang, S.N.; Hsieh, C.H.; Yeh, C.Y.; Grätzel, M. Molecular engineering of push-pull porphyrin dyes for highly efficient dye-sensitized solar cells: The role of benzene spacers. *Angew. Chem. Int. Ed.* **2014**, *53*, 2973–2977. [CrossRef] [PubMed]

12. Han, L.; Islam, A.; Chen, H.; Malapaka, C.; Chiranjeevi, B.; Zhang, S.; Yang, X.; Yanagida, M. High-efficiency dye-sensitized solar cell with a novel co-adsorbent. *Energy Environ. Sci.* **2012**, *5*, 6057–6060. [CrossRef]

13. Kakiage, K.; Aoyama, Y.; Yano, T.; Otsuka, T.; Kyomen, T.; Unno, M.; Hanaya, M. An achievement of over 12 percent efficiency in an organic dye-sensitized solar cell. *Chem. Commun.* **2014**, *50*, 6379–6381. [CrossRef] [PubMed]

14. Mane, S.B.; Cheng, C.F.; Sutanto, A.A.; Datta, A.; Dutta, A.; Hung, C.H. DA-π-A organic dyes for dye-sensitized solar cells: Effect of π-bridge length between two acceptors on photovoltaic properties. *Tetrahedron* **2015**, *71*, 7977–7984. [CrossRef]

15. Xie, Y.; Tang, Y.; Wu, W.; Wang, Y.; Liu, J.; Li, X.; Tian, H.; Zhu, W.H. Porphyrin cosensitization for a photovoltaic efficiency of 11.5%: A record for non-ruthenium solar cells based on iodine electrolyte. *J. Am. Chem. Soc.* **2015**, *137*, 14055–14058. [CrossRef] [PubMed]

16. Kakiage, K.; Aoyama, Y.; Yano, T.; Oya, K.; Fujisawa, J.I.; Hanaya, M. Highly-efficient dye-sensitized solar cells with collaborative sensitization by silyl-anchor and carboxy-anchor dyes. *Chem. Commun.* **2015**, *51*, 15894–15897. [CrossRef] [PubMed]

17. Murakoshi, K.; Kano, G.; Wada, Y.; Yanagida, S.; Miyazaki, H.; Matsumoto, M.; Murasawa, S. Importance of binding states between photosensitizing molecules and the TiO_2 surface for efficiency in a dye-sensitized solar cell. *J. Electroanal. Chem.* **1995**, *396*, 27–34. [CrossRef]

18. Clifford, J.N.; Palomares, E.; Nazeeruddin, M.K.; Grätzel, M.; Nelson, J.; Li, X.; Long, N.J.; Durrant, J.R. Molecular control of recombination dynamics in dye-sensitized nanocrystalline TiO_2 films: Free energy vs. distance dependence. *J. Am. Chem. Soc.* **2004**, *126*, 5225–5233. [CrossRef] [PubMed]

19. Durrant, J.R.; Haque, S.A.; Palomares, E. Towards optimisation of electron transfer processes in dye sensitised solar cells. *Coord. Chem. Rev.* **2004**, *248*, 1247–1257. [CrossRef]

20. Palomares, E.; Martinez-Diaz, M.V.; Haque, S.A.; Torres, T.; Durrant, J.R. State selective electron injection in non-aggregated titanium phthalocyanine sensitised nanocrystalline TiO_2 films. *Chem. Commun.* **2004**, *18*, 2112–2113. [CrossRef] [PubMed]

21. Ladomenou, K.; Kitsopoulos, T.N.; Sharma, G.D.; Coutsolelos, A.G. The importance of various anchoring groups attached on porphyrins as potential dyes for DSSC applications. *RSC Adv.* **2014**, *4*, 21379–21404. [CrossRef]

22. Abbotto, A.; Manfredi, N.; Marinzi, C.; de Angelis, F.; Mosconi, E.; Yum, J.-H.; Xianxi, Z.; Nazeeruddin, M.K.; Grätzel, M. Di-branched di-anchoring organic dyes for dye-sensitized solar cells. *Energy Environ. Sci.* **2009**, *2*, 1094–1101. [CrossRef]

23. Garcia-Iglesias, M.; Yum, J.-H.; Humphry-Baker, R.; Zakeeruddin, S.M.; Pechy, P.; Vazquez, P.; Palomares, E.; Gratzel, M.; Nazeeruddin, M.K.; Torres, T. Effect of anchoring groups in zinc phthalocyanine on the dye-sensitized solar cell performance and stability. *Chem. Sci.* **2011**, *2*, 1145–1150. [CrossRef]

24. Ma, T.; Inoue, K.; Yao, K.; Noma, H.; Shuji, T.; Abe, E.; Yu, J.; Wang, X.; Zhang, B. Photoelectrochemical properties of TiO_2 electrodes sensitized by porphyrin derivatives with different numbers of carboxyl groups. *J. Electroanal. Chem.* **2002**, *537*, 31–38. [CrossRef]

25. Odobel, F.; Blart, E.; Lagree, M.; Villieras, M.; Boujtita, H.; el Murr, N.; Caramori, S.; Alberto Bignozzi, C. Porphyrin dyes for TiO_2 sensitization. *J. Mater. Chem.* **2003**, *13*, 502–510. [CrossRef]

26. Gou, F.; Jiang, X.; Fang, R.; Jing, H.; Zhu, Z. Strategy to improve photovoltaic performance of dssc sensitized by zinc prophyrin using salicylic acid as a tridentate anchoring group. *ACS Appl. Mater. Interfaces* **2014**, *6*, 6697–6703. [CrossRef] [PubMed]

27. Sakurada, T.; Arai, Y.; Segawa, H. Porphyrins with β-acetylene-bridged functional groups for efficient dye-sensitized solar cells. *RSC Adv.* **2014**, *4*, 13201–13204. [CrossRef]

28. Ishida, M.; Hwang, D.; Zhang, Z.; Choi, Y.J.; Oh, J.; Lynch, V.M.; Kim, D.Y.; Sessler, J.L.; Kim, D. β-functionalized push-pull porphyrin sensitizers in dye-sensitized solar cells: Effect of π-conjugated spacers. *ChemSusChem* **2015**, *8*, 2967–2977. [CrossRef] [PubMed]

29. Zhang, T.; Qian, X.; Zhang, P.F.; Zhu, Y.Z.; Zheng, J.Y. A meso-meso directly linked porphyrin dimer-based double D-π-A sensitizer for efficient dye-sensitized solar cells. *Chem. Commun.* **2015**, *51*, 3782–3785. [CrossRef] [PubMed]

30. Higashino, T.; Fujimori, Y.; Sugiura, K.; Tsuji, Y.; Ito, S.; Imahori, H. Synthesis of push-pull porphyrin with two electron-donating and two electron-withdrawing groups and its application to dye-sensitized solar cell. *J. Porphyr. Phthalocyanines* **2015**, *19*, 140–149. [CrossRef]

31. Ambre, R.; Yu, C.Y.; Mane, S.B.; Yao, C.F.; Hung, C.H. Toward carboxylate group functionalized A$_4$, A$_2$B$_2$, A$_3$B oxaporphyrins and zinc complex of oxaporphyrins. *Tetrahedron* **2011**, *67*, 4680–4688. [CrossRef]

32. Ambre, R.; Chen, K.B.; Yao, C.F.; Luo, L.; Diau, E.W.G.; Hung, C.H. Effects of porphyrinic meso-substituents on the photovoltaic performance of dye-sensitized solar cells: Number and position of *p*-carboxyphenyl and thienyl groups on zinc porphyrins. *J. Phys. Chem. C* **2012**, *116*, 11907–11916. [CrossRef]

33. Mane, S.B.; Hu, J.Y.; Chang, Y.C.; Luo, L.; Diau, E.W.G.; Hung, C.H. Novel expanded porphyrin sensitized solar cells using boryl oxasmaragdyrin as the sensitizer. *Chem. Commun.* **2013**, *49*, 6882–6884. [CrossRef] [PubMed]

34. Mane, S.B.; Hung, C.H. Synthesis of carboxylate functionalized A$_3$B and A$_2$B$_2$ thiaporphyrins and their application in dye-sensitized solar cells. *New J. Chem.* **2014**, *38*, 3960–3972. [CrossRef]

35. Mane, S.B.; Luo, L.; Chang, G.F.; Diau, E.W.G.; Hung, C.H. Effects of core-modification on porphyrin sensitizers to the efficiencies of dye-sensitized solar cells. *J. Chin. Chem. Soc.* **2014**, *61*, 545–555. [CrossRef]

36. Luo, L.; Ambre, R.B.; Mane, S.B.; Diau, E.W.G.; Hung, C.H. The *cis*-isomer performs better than the trans-isomer in porphyrin-sensitized solar cells: Interfacial electron transport and charge recombination investigations. *Phys. Chem. Chem. Phys.* **2015**, *17*, 20134–20143. [CrossRef] [PubMed]

37. Mane, S.B.; Hung, C.H. Molecular engineering of boryl oxasmaragdyrins through peripheral modification: Structure–efficiency relationship. *Chem. A Eur. J.* **2015**, *21*, 4825–4841. [CrossRef] [PubMed]

38. Mane, S.B.; Luo, L.; Tsai, H.H.; Hung, C.H. Co-sensitization of free-base and zinc porphyrins: An effective approach to improve the photon-to-current conversion efficiency of dye-sensitized solar cells. *J. Porphyr. Phthalocyanines* **2015**, *19*, 695–707. [CrossRef]

39. Ambre, R.B.; Chang, G.F.; Zanwar, M.R.; Yao, C.F.; Diau, E.W.G.; Hung, C.H. New dual donor-acceptor (2d-π-2a) porphyrin sensitizers for stable and cost-effective dye-sensitized solar cells. *Chem. Asian J.* **2013**, *8*, 2144–2153. [CrossRef] [PubMed]

40. Ambre, R.B.; Chang, G.F.; Hung, C.H. Three *p*-carboxyphenyl groups possessing zinc porphyrins: Efficient, stable, and cost-effective sensitizers for dye-sensitized solar cells. *Chem. Commun.* **2014**, *50*, 725–727. [CrossRef] [PubMed]

41. Ambre, R.B.; Mane, S.B.; Chang, G.F.; Hung, C.H. Effects of number and position of meta and para carboxyphenyl groups of zinc porphyrins in dye-sensitized solar cells: Structure–performance relationship. *ACS Appl. Mater. Interfaces* **2015**, *7*, 1879–1891. [CrossRef] [PubMed]

42. Zervaki, G.E.; Roy, M.S.; Panda, M.K.; Angaridis, P.A.; Chrissos, E.; Sharma, G.D.; Coutsolelos, A.G. Efficient sensitization of dye-sensitized solar cells by novel triazine-bridged porphyrin-porphyrin dyads. *Inorg. Chem.* **2013**, *52*, 9813–9825. [CrossRef] [PubMed]

43. Zervaki, G.E.; Papastamatakis, E.; Angaridis, P.A.; Nikolaou, V.; Singh, M.; Kurchania, R.; Kitsopoulos, T.N.; Sharma, G.D.; Coutsolelos, A.G. A propeller-shaped, triazine-linked porphyrin triad as efficient sensitizer for dye-sensitized solar cells. *Eur. J. Inorg. Chem.* **2014**, *2014*, 1020–1033. [CrossRef]

44. Narra, V.K.; Ullah, H.; Singh, V.K.; Giribabu, L.; Senthilarasu, S.; Karazhanov, S.Z.; Tahir, A.A.; Mallick, T.K.; Upadhyaya, H.M. D-π-a system based on zinc porphyrin dyes for dye-sensitized solar cells: Combined experimental and DFT-TDDFT study. *Polyhedron* **2015**, *100*, 313–320. [CrossRef]